Available online at www.sciencedirect.com

SciVerse ScienceDirect

Procedia Computer Science 18 (2013) 2167 – 2176

Procedia Computer Science

International Conference on Computational Science, ICCS 2013

Numerical analysis of finite element method for a transient two-phase transport model of polymer electrolyte fuel cell

Yuzhou Sun[a], Mingyan He[b], Pengtao Sun[a,*]

[a] *Department of Mathematical Sciences, University of Nevada Las Vegas, 4505 Maryland Parkway, Las Vegas, NV 89154, USA*
[b] *Department of Mathematics, Tongji University, Shanghai, 200092, P.R. China*

Abstract

In this paper, we study a 2D transient two-phase transport model for water species in the cathode gas diffusion layer of hydrogen polymer electrolyte fuel cell (PEFC), the reformulation of water concentration equation is described by using Kirchhoff transformation, and its numerical efficiency is demonstrated by successfully dealing with the discontinuous and degenerate water diffusivity. The semi-discrete and fully discrete finite element approximations with Crank-Nicolson scheme are developed for the present model and the optimal error estimate in H^1 norm and the sub-optimal error estimate in L^2 norm are established for both finite element schemes.

Keywords: Transient two-phase transport model, polymer electrolyte fuel cell (PEFC), Kirchhoff transformation, finite element method, the optimal error estimate, Crank-Nicolson scheme.

1. Introduction

Fuel cells have been used in a large number of industries worldwide because of their advantages such as low environmental impact, rapid start-up and high power density. Polymer electrolyte fuel cells (PEFCs) is presently considered as a potential type of fuel cells for such application. Since PEFCs simultaneously involve electrochemical reactions, current distribution, two-phase flow transport and heat transfer, an extensive mathematical modeling of multi-physics system combined with the advanced numerical techniques shall make a significant impact in gaining a fundamental understanding of the interacting electrochemical and transport phenomena and providing a computer-aided tool for the design and optimization of future fuel cell engines.

Figure 1 schematically shows a single PEFC. A typical PEFC consists of several distinct components [1]: the membrane electrode assembly (MEA) comprised of a proton conducting electrolyte membrane sandwiched between two catalyst layers (CL), the porous gas diffusion layers (GDL), and the bipolar plates with embedded gas channels. In the anode CL, the hydrogen oxidation reaction (HOR) splits the hydrogen into electrons, which are transmitted via the external circuit, and protons, which migrate through the membrane and participate in the oxygen reduction reaction (ORR) in the cathode CL to recombine with oxygen and produce water and waste heat. Inside the PEFCs, water management is a key issue, and is a significant technical challenge. Sufficient amount of water is needed in the

*Corresponding author

Email addresses: suny5@unlv.nevada.edu (Yuzhou Sun), hemingyan1985@yahoo.com.cn (Mingyan He), pengtao.sun@unlv.edu (Pengtao Sun)

Selection and peer review under responsibility of the organizers of the 2013 International Conference on Computational Science
doi:10.1016/j.procs.2013.05.387

membrane to maintain high proton conductivity, however, excess liquid water in the electrode can cause water flooding, and hinder the transport of the reactant from the gas channels to the catalyst layers. It is referred to as balancing membrane hydration with flooding avoidance. Due to such complicated electrochemical reaction and multicomponent and multiphase transport process, mathematical modeling and numerical simulation have become an important tool for the design and optimization of PEFCs [2, 3, 4, 5, 6, 7, 8]. Since there are two important and also conflicting needs in PEFCs: to hydrate the polymer electrolyte and to avoid flooding in porous electrodes and GDL for reactant/product transport, in order to focus on the most important issue in PEFCs - water management, we only consider water transport phenomenon in this paper, model its two-phase transport equation and analyze its finite element approximation. Other species transport phenomena in PEFCs will be studied in a future paper.

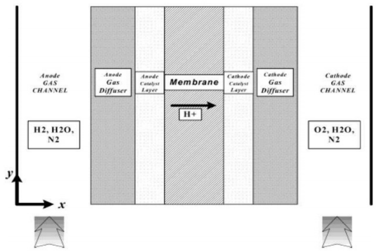

Figure 1: Schematic diagram of a polymer exchange membrane fuel cell

Comparing to the plentiful literature on modeling and experimental study of fuel cells, less works are contributed to the efficient numerical methodology of two-phase transport PEFC model. P. Sun et al [9, 10, 11, 12, 13] lead the field in numerical studies for PEFC due to the cutting edge work on the efficient numerical techniques for the multiphase mixture (M^2) model of PEFC, where, finite element method is adopted to discretize the governing equations of PEFC model, and Kirchhoff transformation [14, 15, 16, 11, 12] is employed to specifically handle the derived discontinuous and degenerate water diffusivity arising in the two-phase water transport model of PEFC with the intention to accelerate the nonlinear iteration and obtain an accurate solution. However, the error estimates of finite element method with Kirchhoff transformation have not been discussed yet for either steady state or transient PEFC model in these papers. The goal of this paper is to accurately analyze the error estimates of the semi-discrete finite element scheme and fully discrete finite element method with Crank-Nicolson scheme for a simplified transient two-phase transport model in the cathode gas diffusion layer (GDL) of PEFC. We finally obtain the optimal error estimate in H^1 norm and the sub-optimal error estimate in L^2 norm for both finite element schemes in spatial discretization, and second order approximation in temporal discretization for the fully discrete scheme.

The rest of this paper is organized as follows. In Section 2, a simplified 2D two-phase transport model in the cathode GDL of PEFC is studied. Then Kirchhoff transformation is introduced to describe the reformulated water concentration equation, and its efficiency is demonstrated on dealing with the discontinuous and degenerate diffusivity. The semi-discrete finite element scheme is presented and its error estimate is given in Section 3. A fully discrete finite element method with Crank-Nicolson scheme is designed and analyzed correspondingly in Section 4.

2. A Simplified 2D Transient Two-phase Transport Model in the Cathode GDL of PEFC

2.1. Model Descriptions

In this section, the governing equations for a simplified 2D transient two-phase transport problem in the cathode GDL of PEFC are described, together with the computational domain and the corresponding boundary conditions.

2.1.1. Governing Equations

To define a simplified 2D transient isothermal two-phase transport model in the cathode GDL, we only need to address a pressure equation using Darcy's law, and water concentration equation in which Darcy's velocity is used. As mentioned in the introduction, water management is the most important and challenging problem in PEFC model. The physical feature of water determines that the two-phase zone and the single-phase zone are co-existing. Nevertheless, GDL is the major component in PEFC that contains both liquid water and gaseous water vapor, while gas channel only contains water vapor. Therefore, in this paper the attention is put on the water species only in GDL instead of all species spreading everywhere. Based on the M^2 model, the two-phase transport model is defined as follows with respect to water's molar concentration C and pressure p [11, 17]:

$$\begin{cases} \epsilon \frac{\partial C}{\partial t} - \nabla \cdot (D(C)\nabla C) + \nabla \cdot (\gamma_c \vec{u} C) & = 0, \\ \nabla \cdot \left(\frac{K}{\epsilon \nu} \nabla p \right) & = 0, \end{cases} \tag{1}$$

where ϵ is the porosity of GDL, the Darcy's velocity $\vec{u}$ is defined as $\vec{u} = -\frac{K}{\epsilon \rho \nu} \nabla p$. We assume $\nabla \cdot \vec{u} = 0$, thus the pressure equation in (1) is introduced. The diffusivity $D(C)$ in GDL is defined as

$$D(C) = \begin{cases} D_g f(\epsilon), & \text{if } C < C_{sat}, \\ \left(\frac{C_{sat}}{\rho_g} - \frac{1}{M} \right) \Gamma_{capdiff}, & \text{if } C \geq C_{sat}, \end{cases} \tag{2}$$

where D_g is the effective water vapor diffusivity given as a constant for isothermal model, and $f(\epsilon) = \epsilon^{1.5}$. The capillary diffusion coefficient $\Gamma_{capdiff} = \frac{M}{\rho_l - C_{sat} M} \frac{\lambda_l \lambda_g}{\nu} \sigma \cos \theta_c (\epsilon K)^{\frac{1}{2}} \frac{dJ(s)}{ds}$. γ_c is the advection correction factor, given as

$$\gamma_c = \begin{cases} 1, & \text{if } C < C_{sat}, \\ \frac{\rho}{C} \left(\frac{\lambda_l}{M} + \frac{\lambda_g}{\rho_g} C_{sat} \right), & \text{if } C \geq C_{sat}, \end{cases} \tag{3}$$

where λ_g and λ_l are the relative mobilities of liquid and gaseous phases defined in Table 1. C_{sat} is the saturated water concentration which is a constant in isothermal case. $J(s)$ is the Leverett function defined as

$$J(s) = \begin{cases} 1.417(1-s) - 2.120(1-s)^2 + 1.263(1-s)^3, & \text{if } \theta_c < 90°, \\ 1.417s - 2.120s^2 + 1.263s^3, & \text{if } \theta_c > 90°, \end{cases} \tag{4}$$

here $s \in [0, 1]$ denotes the liquid saturation, which has coequality with water concentration, shown as $s = \frac{C - Csat}{\frac{\rho_l}{M} - Csat}$. It is not difficult to see $\Gamma_{capdiff} = 0$ when $C = C_{sat}$. Therefore $D(C)$ degenerates at C_{sat}. We define a new advection correction factor $\bar{\gamma}_c = -\frac{K\gamma_c}{\epsilon \rho \nu}$, then the water concentration equation in (1) can be written as

$$\epsilon \frac{\partial C}{\partial t} - \nabla \cdot (D(C)\nabla C) + \nabla \cdot (\bar{\gamma}_c \nabla p C) = 0, \tag{5}$$

Table 1: Parameters and their physical relations [1]

Density	$\rho = \rho_l s + \rho_g (1-s)$
Molar concentration	$C = C_l s + C_g (1-s)$
Kinematic viscosity	$\nu = \left(\frac{k_{rl}}{\nu_l} + \frac{k_{rg}}{\nu_g} \right)^{-1}$
Relative mobilities	$\lambda_l(s) = \frac{k_{rl}/\nu_l}{k_{rl}/\nu_l + k_{rg}/\nu_g}$, $\lambda_g(s) = 1 - \lambda_l(s)$
Relative permeabilities	$k_{rl} = s^3$, $k_{rg} = (1-s)^3$

2.1.2. Computational Domain and Boundary Conditions

The governing equations (1) take place in the cathode GDL of PEFC, as shown in Fig. 2. The x-axis represents the flow direction and the y-axis points in the through-plane direction. The dimension sizes of this computational domain are marked in Fig. 2 as well. $\frac{\partial C}{\partial n} = 0$ and $\frac{\partial p}{\partial n} = 0$ on the left and right walls ($\partial \Omega_2$ and $\partial \Omega_3$). On the bottom wall connecting with gas channel ($\partial \Omega_1$), C is given as constant C_b and $p(x) = p_1 - (p_1 - p_2)\frac{x}{l_{\text{PEFC}}}$. On the top wall connecting with catalyst layer ($\partial \Omega_4$), $\frac{\partial p}{\partial n} = 0$ and $D(C)\nabla C \cdot \vec{n} - (\bar{\gamma}_c \nabla p C) \cdot \vec{n} = \frac{I(x)}{2F}$, where F is the Faraday constant and $I(x)$ the volumetric transfer current density of reaction, given as [11] $I(x) = \left(I_1 - (I_1 - I_2)\frac{x}{l_{\text{PEFC}}} \right)$. Here p_1, p_2, I_1 and I_2 are predetermined constants. In fact, $I(x)$ is the linear reduction of Butler-Volmer equation, indicating that the transfer current density linearly decreases from the inlet to the outlet.

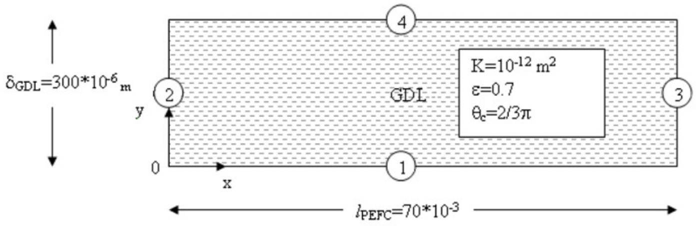

Figure 2: Computational Domain

2.2. Reformulation of Water Equation by Kirchhoff Transformation

2.2.1. Kirchhoff Transformation

As discussed in section 2.1.1, $D(C)$ is degenerate and also discontinuous at C_{sat}, which causes the numerical simulation to be inefficient and unstable. In order to resolve such computational difficulties, we introduce the Kirchhoff transformation [11] as $W(C) = \int_0^C D(w)dw$. Then

$$W(C) = \begin{cases} D_g f(\epsilon)C, & \text{if } C < C_{sat}, \\ D_g f(\epsilon)C_{sat} + \int_{C_{sat}}^{C} \left(\frac{C_{sat}}{\rho_g} - \frac{1}{M}\right)\Gamma_{capdiff}dw, & \text{if } C \geq C_{sat}. \end{cases} \tag{6}$$

Furthermore,

$$\Delta W(C) = \nabla \cdot (D(C)\nabla C) = \begin{cases} \nabla \cdot (D_g f(\epsilon)\nabla C), & \text{if } C < C_{sat}, \\ \nabla \cdot \left(\left(\frac{C_{sat}}{\rho_g} - \frac{1}{M}\right)\Gamma_{capdiff}\nabla C\right), & \text{if } C \geq C_{sat}. \end{cases} \tag{7}$$

Thus we are able to reformulate the water concentration equation (5) with Kirchhoff transformation as follows

$$\begin{cases} \frac{\epsilon}{D(C)+\delta}\frac{\partial W}{\partial t} - \Delta W = -\nabla \cdot (\bar{\gamma}_c \nabla pC) & \text{in GDL}, \\ W = \int_0^{C_b} D(w)dw & \text{on } \partial\Omega_1, \\ \frac{\partial W}{\partial n} = 0 & \text{on } \partial\Omega_2, \partial\Omega_3, \\ \nabla W \cdot \vec{n} - \bar{\gamma}_c \nabla pC(W) \cdot \vec{n} = \frac{I(x)}{2F} & \text{on } \partial\Omega_4. \end{cases} \tag{8}$$

Here δ is a sufficiently small positive number for the sake of avoidance of possible zero denominator at $C = C_{\text{sat}}$.

It may be improper if one insists on applying Kirchhoff transformation to $\nabla \cdot (\bar{\gamma}_c \nabla pC)$, a new convection term that explicitly depends on W will be obtained as

$$\nabla \cdot (\bar{\gamma}_c \nabla pC) = \bar{\gamma}_c \nabla p \cdot \nabla C + \nabla \cdot (\bar{\gamma}_c \nabla p)C = \bar{\gamma}_c \nabla p \cdot \frac{\nabla W}{D(C)} + \nabla \cdot (\bar{\gamma}_c \nabla p)C(W), \tag{9}$$

then the corresponding reformulated water concentration equation becomes

$$\frac{\epsilon}{D(C)+\delta}\frac{\partial W}{\partial t} - \Delta W + \frac{\bar{\gamma}_c \nabla p}{D(C)+\delta} \cdot \nabla W = -\nabla \cdot (\bar{\gamma}_c \nabla p)C(W), \tag{10}$$

where, a huge convection term may be produced when the water concentration C is close to the degenerate point C_{sat}. Therefore, for the interest of numerical stability, it is better to avoid applying Kirchhoff transformation to the convection term in (8), and leave it to the right hand side as an equivalent force term in order to achieve a stable numerical simulation.

2.2.2. Model Generalization

In order to extend the numerical analysis on error estimates of finite element method, which will be given in Section 3, to a more general case, the reformulated water concentration equation can be generalized to the following form of convection-diffusion-reaction equation

$$r(C)\frac{\partial W}{\partial t} - \Delta W + \vec{b}(C, \nabla p) \cdot \nabla W = f(C, \nabla p, \Delta p), \tag{11}$$

where $r(C) = \frac{\epsilon}{D(C)+\delta}$, $\vec{b}(C, \nabla p) = \frac{\bar{\gamma}_c \nabla p}{D(C)+\delta}$, $f(C, \nabla p, \Delta p) = -\nabla \cdot (\bar{\gamma}_c \nabla p)\, C(W)$. Obviously, (8) and (10) are just special cases of (11). Without loss of generality, in what follows, we will carry out the error estimates of finite element method for (11) instead of (8) or (10).

All the necessary coefficient functions and their proper derivatives are Lipschitz continuous, and their upper and lower bounds satisfy the following conditions for $C \geq 0$,

$$d \leq D(C) \leq D, 0 < r \leq r(C) \leq R, b < \vec{b}(C, \nabla p) < B, |\gamma(C)| < \Gamma, b_p < \left|\vec{b}_p(C, \nabla p)\right| < B_p, b_{pp} < \left|\vec{b}_{pp}(C, \nabla p)\right| < B_{pp}. \quad (12)$$

However, since $D(C)$ is discontinuous at C_{sat}, $r(C)$ and $\vec{b}(C, \nabla p)$ are also discontinuous at C_{sat} for (8). Therefore the following conditions are to be satisfied when C is on either side of C_{sat},

$$\left|r'(C)\right| \leq R',\ \left|r''(C)\right| \leq R'',\ b_c < \left|\vec{b}_c(C, \nabla p)\right| < B_c, b_{cc} < \left|\vec{b}_{cc}(C, \nabla p)\right| < B_{cc},\ b_{cp} < \left|\vec{b}_{cp}(C, \nabla p)\right| < B_{cp}. \quad (13)$$

2.2.3. Kirchhoff Inverse Transformation

According to the definition of Kirchhoff transformation in (6), the expression for C is not explicit. For the case $C < C_{sat}$, since the Kirchhoff transformation is linear, it is not hard to calculate C directly from W using

$$C = \left(D_g f(\epsilon)\right)^{-1} W. \quad (14)$$

However, if $C \geq C_{sat}$, it is necessary to adopt Newton's method to find a proper C, given by the following iterative solution [11]($k = 0, 1, 2, \ldots$):

$$C_{k+1} = C_k + \frac{W - D_g f(\epsilon) C_{sat} - \int_{C_{sat}}^{C_k} D(w)dw}{D(C_k) + \delta}. \quad (15)$$

3. Semi-discrete Scheme and Its Error Estimate

3.1. Semi-discrete FEM

After applying Kirchhoff transformation, the governing equations (5) now become:

$$\begin{cases} \frac{\epsilon}{D(C)+\delta}\frac{\partial W}{\partial t} - \Delta W &= -\nabla \cdot (\bar{\gamma}_c \nabla p C), \\ \nabla \cdot \left(\frac{K}{\epsilon \nu} \nabla p\right) &= 0. \end{cases} \quad (16)$$

Define $H_w = \left\{W \in H^1\left(0, T; H^{k+1}(\Omega) \cap W^{1,\infty}(\Omega)\right); W|_{\partial\Omega_1} = C_b\right\}$, $\bar{H}_w = \{W \in H_w; W|_{\partial\Omega} = 0\}$, $H_p = \left\{p \in H^{k+1}(\Omega) \cap W^{1,\infty}(\Omega); p|_{\partial\Omega_1} = p_1 - (p_1 - p_2)\frac{x}{l_{\text{PEFC}}}\right\}$ and $\bar{H}_p = \left\{p \in H_p; p|_{\partial\Omega} = 0\right\}$ and apply standard finite element method to (16).

The weak form of (16) is given as: find $(W, p) \in H_w \times H_p$, such that for any $(v, q) \in H_w \times H_p$:

$$\begin{cases} \left(\frac{\epsilon}{D(C)+\delta}\frac{\partial W}{\partial t}, v\right) + (\nabla W, \nabla v) = (\bar{\gamma}_c \nabla p C, \nabla v) + \int_{\Omega_4} \frac{I(x)}{2F} v ds, \\ \left(\frac{K}{\epsilon \nu}\nabla p, \nabla q\right) = 0. \end{cases} \quad (17)$$

Define piecewise linear polynomial finite element spaces, $S_h \subseteq H_w$, $T_h \subseteq H_p$, $\bar{S}_h \subseteq \bar{H}_w$ and $\bar{T}_h \subseteq \bar{H}_p$. Given $C_h^n \in S_h$, find $(W_h^{n+1}, p_h^{n+1}) \in S_h \times T_h$ such that for any $(v_h, q_h) \in \bar{S}_h \times \bar{T}_h$,

$$\begin{cases} \left(\frac{\epsilon}{D(C_h^n)+\delta}\frac{\partial W_h^{n+1}}{\partial t}, v_h\right) + \left(\nabla W_h^{n+1}, \nabla v_h\right) = \left(\bar{\gamma}_c \nabla p C_h^n, \nabla v_h\right) + \int_{\Omega_4} \frac{I(x)}{2F} v_h ds, \\ \left(\frac{K}{\epsilon \nu}\nabla p_h^{n+1}, \nabla q_h\right) = 0. \end{cases} \quad (18)$$

3.2. FEM Approximation Analysis

Lemma 3.1. *[18] Suppose $p \in H^{k+1}(\Omega)$, then*

$$\|p - p_h\|_{L^\infty(L^2)} + h\|p - p_h\|_{L^\infty(H^1)} \le Kh^{k+1}\|p\|_{L^\infty(H^{k+1})}. \tag{19}$$

Lemma 3.2. *Suppose $C \in H^1\left(0, T; H^{k+1}(\Omega) \cap W^{1,\infty}(\Omega)\right)$ and $W = \int_0^C D(w)dw$. The norms of C and W have the relation*

$$d\|C\|_{H^{k+1}\cap W^{1,\infty}} \le \|W\|_{H^{k+1}\cap W^{1,\infty}} \le D\|C\|_{H^{k+1}\cap W^{1,\infty}}. \tag{20}$$

Proof. Since $W = \int_0^C D(w)dw$, by taking derivatives with respect to time and space respectively, one has $W_t = D(C)C_t$ and $\nabla W = D(C)\nabla C$. Because $d \le D(C) \le D$, (20) can be obtained easily. □

Apply the standard finite element method to (11) for the purpose of error estimate, its weak form is given as: find $C, W \in H_w$, such that

$$\left(r(C)\frac{\partial W}{\partial t}, v\right) + (\nabla W, \nabla v) + (\vec{b}(C, \nabla p)\cdot\nabla W, v) = (f(C, \nabla p, \Delta p), v),\ \forall v \in \bar{H}_w. \tag{21}$$

The semi-discretization form of (11) is given as follows: Find $C_h, W_h \in S_h$, such that

$$\left(r(C_h)\frac{\partial W_h}{\partial t}, v_h\right) + (\nabla W_h, \nabla v_h) + (\vec{b}(C_h, \nabla p_h)\cdot\nabla W_h, v_h) = (f(C_h, \nabla p_h, \Delta p_h), v_h),\ \forall v_h \in \bar{S}_h. \tag{22}$$

Define a projection $\tilde{W} \in S_h$ to satisfy

$$(\nabla(W - \tilde{W}), \nabla v_h) + (\vec{b}(C, \nabla p)\cdot\nabla(W - \tilde{W}), v_h) = 0,\ \forall v_h \in \bar{S}_h, \tag{23}$$

then (21) becomes: Find $C, W \in H_w$, such that

$$\left(r(C)\frac{\partial W}{\partial t}, v\right) + (\nabla\tilde{W}, \nabla v) + (\vec{b}(C, \nabla p)\cdot\nabla\tilde{W}, v) = (f(C, \nabla p, \Delta p), v),\ \forall v \in \bar{H}_w. \tag{24}$$

Lemma 3.3. *Suppose $C \in H^1\left(0, T; H^{k+1}(\Omega) \cap W^{1,\infty}(\Omega)\right)$ and $W = \int_0^C D(w)dw$. Let $\tilde{W}$ be the projection defined in (23), then the error estimates for projections are given as*

$$\left\|W - \tilde{W}\right\|_0 + h\left\|W - \tilde{W}\right\|_1 \le Kh^{k+1}\|C\|_{k+1}, \tag{25}$$

$$\left\|(W - \tilde{W})_t\right\|_0 + h\left\|(W - \tilde{W})_t\right\|_1 \le Kh^{k+1}(\|C\|_{k+1} + \|C_t\|_{k+1}). \tag{26}$$

Proof. Let $\Pi_h W \in \bar{S}_h$ be the interpolation of W and $W - \tilde{W} = W - \Pi_h W + \Pi_h W - \tilde{W}$. Since $\Pi_h W - \tilde{W} \in \bar{S}_h$, by (23),

$$\begin{aligned}&\left(\nabla\left(W - \tilde{W}\right), \nabla\left(W - \tilde{W}\right)\right) + \left(\vec{b}(C, \nabla p)\cdot\nabla\left(W - \tilde{W}\right), W - \tilde{W}\right)\\ &= \left(\nabla\left(W - \tilde{W}\right), \nabla(W - \Pi_h W)\right) + \left(\vec{b}(C, \nabla p)\cdot\nabla\left(W - \tilde{W}\right), W - \Pi_h W\right).\end{aligned} \tag{27}$$

By (12), $\left\|\nabla\left(W - \tilde{W}\right)\right\|_0 + \left\|W - \tilde{W}\right\|_0 \le K(\|\nabla(W - \Pi_h W)\|_0 + \|W - \Pi_h W\|_0)$, where K is a proper constant. This implies

$$\left\|W - \tilde{W}\right\|_1 \le K \inf_{\Pi_h W \in \bar{S}_h}\|W - \Pi_h W\|_1 \le Kh^k\|W\|_{k+1} \le Kh^k\|C\|_{k+1}. \tag{28}$$

Let $e = W - \tilde{W}$, $e \in \bar{S}_h$, define $w \in H^2(\Omega) \cap H_0^1(\Omega)$ to satisfy the adjoint problem of (23):

$$\begin{cases} -\Delta w - \nabla(\vec{b}(C, \nabla p)\cdot w) = e,\\ w = 0.\end{cases} \tag{29}$$

Then

$$\|e\|_0^2 = -(e,\Delta w) - \left(e, \nabla(\vec{b}(C,\nabla p)\cdot w)\right) = (\nabla e, \nabla(w - \Pi_h w + \Pi_h w)) + \left(\nabla e, \vec{b}(C,\nabla p)\cdot(w - \Pi_h w + \Pi_h w)\right)$$
$$= (\nabla e, \nabla(w-\Pi_h w)) - \left(\nabla e, \vec{b}(C,\nabla p)\cdot(w-\Pi_h w)\right) \le K\|e\|_1 \|w-\Pi_h w\|_1, \tag{30}$$

where $\Pi_h w$ is the interpolation of w with $\Pi_h w \in \bar{S}_h$, and K is a constant. Since $\|w-\Pi_h w\|_1 \le Kh\|w\|_2$ and $\|w\|_2 \le \|e\|_0$, it is easy to see that $\|e\|_0^2 \le Kh\|e\|_1\|e\|_0$. Therefore by (28) and Lemma 3.2,

$$\left\|W-\tilde{W}\right\|_0 \le Kh\left\|W-\tilde{W}\right\|_1 \le Kh^{k+1}\|W\|_{k+1} \le Kh^{k+1}\|C\|_{k+1}. \tag{31}$$

Take the derivative with respect to t in (23),

$$\left(\nabla(W-\tilde{W})_t, \nabla v_h\right) + \left(\vec{b}_t(C,\nabla p)\cdot\nabla(W-\tilde{W}), v_h\right) + \left(\vec{b}(C,\nabla p)\cdot\nabla(W-\tilde{W})_t, v_h\right) = 0, \tag{32}$$

(26) can be obtained similarly.

□

Lemma 3.4. *Suppose* $C \in H^1\left(0,T;H^{k+1}(\Omega)\cap W^{1,\infty}(\Omega)\right)$ *and* $W = \int_0^C D(w)dw$. *Let* $\tilde{W}$ *be the projection defined in (23). Then* W *has the following error estimate result:*

$$\left\|W-\tilde{W}\right\|_{1,\infty} \le K\left(1+|\ln h|^{\frac{3}{2}}\right)h^{k-\frac{n}{2}}\|C\|_{k+1}. \tag{33}$$

Proof. Define a projection operator P_h to satisfy $\tilde{W} = P_h W \in \bar{S}_h$, then by (23), $W-\tilde{W} = W - P_h W = (I-P_h)W = (I-P_h)(W-\Pi_h W)$, where I is the identity operator and $P_h\Pi_h W = \Pi_h W$. Since $|\ln h|^{-\frac{1}{2}}\|P_h W\|_{0,\infty} + h|P_h W|_{1,\infty} \le K\left(\|W\|_{0,\infty} + h|\ln h||W|_{1,\infty}\right)$ (see [18]), one can obtain

$$\left\|W-\tilde{W}\right\|_{0,\infty} \le \left(K|\ln h|^{\frac{1}{2}}+1\right)\|W-\Pi_h W\|_{0,\infty} + Kh|\ln h|^{\frac{3}{2}}|W-\Pi_h W|_{1,\infty} \le \left(K|\ln h|^{\frac{3}{2}}+1\right)h^{k+1-\frac{n}{2}}\|W\|_{k+1}, \tag{34}$$

$$h\left|W-\tilde{W}\right|_{1,\infty} \le K\|W-\Pi_h W\|_{0,\infty} + h(1+K|\ln h|)|W-\Pi_h W|_{1,\infty} \le (K|\ln h|+1)h^{k+1-\frac{n}{2}}\|W\|_{k+1}, \tag{35}$$

therefore

$$\left\|W-\tilde{W}\right\|_{1,\infty} \le \left(K|\ln h|^{\frac{3}{2}}+1\right)h^{k-\frac{n}{2}}\|W\|_{k+1} \le \left(K|\ln h|^{\frac{3}{2}}+1\right)h^{k-\frac{n}{2}}\|C\|_{k+1}. \tag{36}$$

□

In order to carry out the optimal approximation order, k is required to be greater than $n-1$ for $n \ge 2$. Especially for the model in this paper, because $n = 2$, it is required for k to be greater than 1, which implies that a second order interpolation should be used.

Corollary 3.1. *Suppose* $C \in H^1\left(0,T;H^{k+1}(\Omega)\cap W^{1,\infty}(\Omega)\right)$ *and* $k > 1$. *Let* $\tilde{W}$ *be the projection defined in (23) and* $W = \int_0^C D(w)dw$. *Then one has the following error estimate:*

$$\left\|\tilde{W}\right\|_\infty + \left\|\nabla\tilde{W}\right\|_\infty + \|W_t\|_{1,\infty} \le K\left(1+|\ln h|^{\frac{3}{2}}\right)h^{k-\frac{n}{2}}. \tag{37}$$

Proof. For $C \in H^1\left(0,T;H^{k+1}(\Omega)\cap W^{1,\infty}(\Omega)\right)$ and $k > 1$, since $n = dim(GDL) = 2$, $\left\|\tilde{W}\right\|_\infty + \left\|\nabla\tilde{W}\right\|_\infty + \|W_t\|_{1,\infty} \le \left\|W-\tilde{W}\right\|_{1,\infty} + \|W\|_{1,\infty} + \|W_t\|_{1,\infty} \le K\left(1+|\ln h|^{\frac{3}{2}}\right)h^{k-\frac{n}{2}}$. □

Let $W - W_h = (W-\tilde{W}) + (\tilde{W}-W_h) = \eta + \xi$ and $v_h = \xi$, the error equation of (11) can be achieved by (24)−(22),

$$\left(r(C_h)\frac{\partial\xi}{\partial t},\xi\right) + \left(r(C_h)\frac{\partial\eta}{\partial t},\xi\right) + \left(r(C)-r(C_h))\frac{\partial W}{\partial t},\xi\right) + (\nabla\xi,\nabla\xi)$$
$$+\left(\left(\vec{b}(C,\nabla p)-\vec{b}(C_h,\nabla p_h)\right)\cdot\nabla\tilde{W},\xi\right) + \left(\vec{b}(C_h,\nabla p_h)\cdot\nabla\xi,\xi\right) = (f(C,\nabla p,\Delta p) - f(C_h,\nabla p_h,\Delta p_h),\xi). \tag{38}$$

Use (12), (13), when C and C_h are both greater than or both less than C_{sat}, $\left|\vec{b}(C,\nabla p)-\vec{b}(C_h,\nabla p_h)\right| \le \left|\vec{b}_c\right| \|C-C_h\|_0 + \left|\vec{b}_p\right| \|\nabla(p-p_h)\|_0 \le K_1 \|C-C_h\|_0 + K_2 h^k \|p\|_{k+1}$, where K_1 and K_2 are constants. When C_{sat} is between C and C_h, $\left|\vec{b}(C,\nabla p)-\vec{b}(C_h,\nabla p_h)\right| \le \left|\vec{b}(C,\nabla p)-\vec{b}(C_{sat},\nabla p_h)\right| + \left|\vec{b}(C_{sat},\nabla p)-\vec{b}(C_h,\nabla p_h)\right| \le \left|\vec{b}_c\right| \|C-C_{sat}\|_0 + \left|\vec{b}_c\right| \|C_{sat}-C_h\|_0 + \left|\vec{b}_p\right| \nabla \|p-p_h\|_0 \le K_1 \|C-C_h\|_0 + K_2 h^k \|p\|_{k+1}$. Without loss of generality, this technique can be applied to r and f as well. Use Hölder's inequality and ϵ-inequality,

$$\begin{aligned}
&|(f(C,\nabla p,\Delta p)-f(C_h,\nabla p_h,\Delta p_h),\xi)| = |-(\nabla\cdot(\gamma(C)\nabla p)\,C-\nabla\cdot(\gamma(C_h)\nabla p_h)\,C_h,\xi)| \\
&\le |(\gamma(C)\nabla p,\nabla(C\xi))-(\gamma(C_h)\nabla(p-p_h),\nabla((C-C_h)\xi))| + |(\gamma(C_h)\nabla(p-p_h),\nabla(C\xi))| \\
&+ |(\gamma(C_h)\nabla p,\nabla((C-C_h)\xi))-(\gamma(C_h)\nabla p,\nabla(C\xi))| \\
&\le K\left(h^{2k}+\|\xi\|_0^2+\epsilon\|\nabla\xi\|_0^2+\|\eta\|_0^2+\|\nabla\eta\|_0^2\right),
\end{aligned} \tag{39}$$

where $C \in H^1\left(0,T;H^{k+1}(\Omega)\cap W^{1,\infty}(\Omega)\right)$ and $p \in H^{k+1}(\Omega)\cap W^{1,\infty}(\Omega)$. Since the first term on the left hand side in (38) can be written as $\int_\Omega r(C_h)\frac{\partial\xi}{\partial t}\xi dx = \int_\Omega r(C_h)\frac{\partial}{\partial t}\left(\frac{1}{2}\xi^2\right)dx = \int_\Omega \frac{\partial}{\partial t}\left(\frac{1}{2}r(C_h)\xi^2\right)dx - \int_\Omega r'(C_h)\frac{\partial C_h}{\partial t}\left(\frac{1}{2}\xi^2\right)dx$, integrate both sides of (38) with respect to t,

$$\|\xi\|_0^2 + \int_0^t \|\nabla\xi\|_0^2 \le K\left(\int_0^t \|\eta\|_0^2 + \int_0^t \|\eta_t\|_0^2 + \int_0^t \|\nabla\eta\|_0^2 + \epsilon\int_0^t \|\nabla\xi\|_0^2 + \int_0^t \|\xi\|_0^2 + h^{2k}\right). \tag{40}$$

The choice of constant K is made possible by Corollary 3.1. Apply Gronwall's inequality to (40), thus,

$$\|\xi\|_{L^\infty(0,T;L^2)} + \|\nabla\xi\|_{L^2(0,T;L^2)} \le K\left(\|\eta\|_{L^2(0,T;L^2)} + \|\eta_t\|_{L^2(0,T;L^2)} + \|\nabla\eta\|_{L^2(0,T;L^2)} + h^k\right), \tag{41}$$

and therefore,

$$\|C-C_h\|_{L^\infty(L^2)} + \|C-C_h\|_{L^2(H^1)} \le \|W-W_h\|_{L^\infty(L^2)} + \|W-W_h\|_{L^2(H^1)} \le Kh^k\left(\|C\|_{L^2(H^{k+1})} + \|C_t\|_{L^2(H^{k+1})}\right). \tag{42}$$

Let $v_h = \xi_t$ in (38), similarly,

$$\|(C-C_h)_t\|_{L^\infty(L^2)} + \|(C-C_h)_t\|_{L^2(H^1)} \le \|(W-W_h)_t\|_{L^\infty(L^2)} + \|(W-W_h)_t\|_{L^2(H^1)} \le Kh^k\left(\|C\|_{L^2(H^{k+1})} + \|C_t\|_{L^2(H^{k+1})}\right). \tag{43}$$

Theorem 3.1. *Suppose $C \in H^1\left(0,T;H^{k+1}(\Omega)\cap W^{1,\infty}(\Omega)\right)$, $p \in H^{k+1}(\Omega)\cap W^{1,\infty}(\Omega)$, $W = \int_0^C D(\omega)d\omega$ and $k > 1$. With (12) and (13), the numerical solution of (11) has error estimates as follows:*

$$\|p-p_h\|_{L^\infty(L^2)} + h\|p-p_h\|_{L^\infty(H^1)} \le Kh^{k+1}\|p\|_{L^\infty(H^{k+1})}, \tag{44}$$

and

$$\|C-C_h\|_{L^\infty(L^2)} + \|C-C_h\|_{L^2(H^1)} + \|(C-C_h)_t\|_{L^\infty(L^2)} + \|(C-C_h)_t\|_{L^2(H^1)} \le Kh^k\left(\|C\|_{L^2(H^{k+1})} + \|C_t\|_{L^2(H^{k+1})}\right). \tag{45}$$

4. Fully Discrete Scheme and Its Error Estimate

4.1. Fully Discretization

In this section, a fully discrete scheme is designed for the model using Crank-Nicolson Scheme and also its error estimate is given.

Define $\varphi_i = \varphi(t_i)$, $\varphi_{i+\frac{1}{2}} = \varphi(t_{i+\frac{1}{2}})$, $\partial_t\varphi^{n+\frac{1}{2}} = \frac{\varphi_{n+1}-\varphi_n}{\Delta t}$ and $\varphi^{n+\frac{1}{2}} = \frac{\varphi_{n+1}+\varphi_n}{2}$, where $0 = t_0 < t_1 < \cdots < t_N = T$, $\Delta t = \frac{T}{N}$, $t_i = i\Delta t$ and $t_{i+\frac{1}{2}} = \left(i+\frac{1}{2}\right)\Delta t$. $(i = 0,1,\cdots,N.)$ Let (21) take value at $t_{n+\frac{1}{2}}$, and the projection defined as (23),

$$\left(r\left(C_{n+\frac{1}{2}}\right)\left(\frac{\partial W}{\partial t}\right)_{n+\frac{1}{2}},v\right) + \left(\nabla\tilde{W}_{n+\frac{1}{2}},\nabla v\right) + \left(\vec{b}\left(C_{n+\frac{1}{2}},\nabla p_{n+\frac{1}{2}}\right)\cdot\nabla\tilde{W}_{n+\frac{1}{2}},v\right) = \left(f\left(C_{n+\frac{1}{2}},\nabla p_{n+\frac{1}{2}},\Delta p_{n+\frac{1}{2}}\right),v\right). \tag{46}$$

Apply Crank-Nicolson Scheme to (11),

$$\left(r\left(C_h^{n+\frac{1}{2}}\right)\partial_t W_h^{n+\frac{1}{2}},v_h\right) + \left(\nabla W_h^{n+\frac{1}{2}},\nabla v_h\right) + \left(\vec{b}\left(C_h^{n+\frac{1}{2}},\nabla p_h^{n+\frac{1}{2}}\right)\cdot\nabla W_h^{n+\frac{1}{2}},v_h\right) = \left(f\left(C_h^{n+\frac{1}{2}},\nabla p_h^{n+\frac{1}{2}},\Delta p_h^{n+\frac{1}{2}}\right),v_h\right). \tag{47}$$

4.2. Error Estimates

The error equation of the discrete scheme described in section 4.1 is achieved by (46)–(47):

$$\left(r\left(C_{n+\frac{1}{2}}\right)\left(\frac{\partial W}{\partial t}\right)_{n+\frac{1}{2}} - r\left(C_h^{n+\frac{1}{2}}\right)\partial_t W_h^{n+\frac{1}{2}}, v_h\right) + \left(\vec{b}\left(C_{n+\frac{1}{2}}, \nabla p_{n+\frac{1}{2}}\right)\cdot\nabla\tilde{W}_{n+\frac{1}{2}} - \vec{b}\left(C_h^{n+\frac{1}{2}}, \nabla p_h^{n+\frac{1}{2}}\right)\cdot\nabla W_h^{n+\frac{1}{2}}, v_h\right)$$
$$+\left(\nabla\tilde{W}_{n+\frac{1}{2}} - \nabla W_h^{n+\frac{1}{2}}, \nabla v_h\right) = \left(f\left(C_{n+\frac{1}{2}}, \nabla p_{n+\frac{1}{2}}, \Delta p_{n+\frac{1}{2}}\right) - f\left(C_h^{n+\frac{1}{2}}, \nabla p_h^{n+\frac{1}{2}}, \Delta p_h^{n+\frac{1}{2}}\right), v_h\right). \quad (48)$$

Use the fact that $W - W_h = W - \tilde{W} + \tilde{W} - W_h = \eta + \xi$, (48) becomes:

$$\sum_1^{11} G_i = \left(\left(r\left(C_{n+\frac{1}{2}}\right) - r\left(C_h^{n+\frac{1}{2}}\right)\right)\left(\frac{\partial W}{\partial t}\right)_{n+\frac{1}{2}}, v_h\right) + \left(r\left(C_h^{n+\frac{1}{2}}\right)\left(\left(\frac{\partial W}{\partial t}\right)_{n+\frac{1}{2}} - \partial_t W^{n+\frac{1}{2}}\right), v_h\right)$$
$$+\left(r\left(C_h^{n+\frac{1}{2}}\right)\left(\partial_t\eta^{n+\frac{1}{2}} - \left(\frac{\partial\eta}{\partial t}\right)_{n+\frac{1}{2}}\right), v_h\right) + \left(r\left(C_h^{n+\frac{1}{2}}\right)\left(\frac{\partial\eta}{\partial t}\right)_{n+\frac{1}{2}}, v_h\right) + \left(r\left(C_h^{n+\frac{1}{2}}\right)\partial_t\xi^{n+\frac{1}{2}}, v_h\right)$$
$$+\left(\nabla\tilde{W}_{n+\frac{1}{2}} - \nabla\tilde{W}^{n+\frac{1}{2}}, \nabla v_h\right) + \left(\nabla\xi^{n+\frac{1}{2}}, \nabla v_h\right) + \left(\left(\vec{b}\left(C_{n+\frac{1}{2}}, \nabla p_{n+\frac{1}{2}}\right) - \vec{b}\left(C_h^{n+\frac{1}{2}}, \nabla p_h^{n+\frac{1}{2}}\right)\right)\cdot\nabla\tilde{W}_{n+\frac{1}{2}}, v_h\right)$$
$$+\left(\vec{b}\left(C_h^{n+\frac{1}{2}}, \nabla p_h^{n+\frac{1}{2}}\right)\cdot\nabla\left(\tilde{W}_{n+\frac{1}{2}} - \tilde{W}^{n+\frac{1}{2}}\right), v_h\right) + \left(\vec{b}\left(C_h^{n+\frac{1}{2}}, \nabla p_h^{n+\frac{1}{2}}\right)\cdot\nabla\xi^{n+\frac{1}{2}}, v_h\right)$$
$$-\left(f\left(C_{n+\frac{1}{2}}, \nabla p_{n+\frac{1}{2}}, \Delta p_{n+\frac{1}{2}}\right) - f\left(C_h^{n+\frac{1}{2}}, \nabla p_h^{n+\frac{1}{2}}, \Delta p_h^{n+\frac{1}{2}}\right), v_h\right) = 0, \quad (49)$$

where G_i is the ith term in (49).

Without loss of generality, let ζ_c be between $C^{n+\frac{1}{2}}$ and $C_h^{n+\frac{1}{2}}$ and ζ_p be between $p^{n+\frac{1}{2}}$ and $p_h^{n+\frac{1}{2}}$. By Taylor's expansion $\left(\frac{\partial\varphi}{\partial t}\right)_{n+\frac{1}{2}} - \partial_t\varphi^{n+\frac{1}{2}} = O(\Delta t)^2|\varphi_{ttt}|$ and $\varphi_{n+\frac{1}{2}} - \varphi^{n+\frac{1}{2}} = O(\Delta t)^2|\varphi_{tt}|$, the following technique is used to G_7:

$$\left|\vec{b}\left(C_{n+\frac{1}{2}}, \nabla p_{n+\frac{1}{2}}\right) - \vec{b}\left(C_h^{n+\frac{1}{2}}, \nabla p_h^{n+\frac{1}{2}}\right)\right| \le \left|\vec{b}\left(C_{n+\frac{1}{2}}, \nabla p_{n+\frac{1}{2}}\right) - \vec{b}\left(C^{n+\frac{1}{2}}, \nabla p^{n+\frac{1}{2}}\right)\right| + \left|\vec{b}\left(C^{n+\frac{1}{2}}, \nabla p^{n+\frac{1}{2}}\right) - \vec{b}\left(C_h^{n+\frac{1}{2}}, \nabla p_h^{n+\frac{1}{2}}\right)\right|$$
$$\le O(\Delta t)^2\left|\vec{b}_{cc}C_t^2 + 2\vec{b}_{cp}C_t\nabla p_t + \vec{b}_{pp}\nabla p_t^2 + \vec{b}_c C_{tt} + \vec{b}_p\nabla p_{tt}\right| + \left|\vec{b}_c\frac{\partial\zeta_c}{\partial C} + \vec{b}_p\frac{\partial\zeta_p}{\partial p}\right|\left(\left\|\xi^{n+\frac{1}{2}} + \eta^{n+\frac{1}{2}}\right\|_0 + \nabla\left\|p^{n+\frac{1}{2}} - p_h^{n+\frac{1}{2}}\right\|_0\right)$$
$$\le K\left(O(\Delta t)^2 + \left\|\xi^{n+\frac{1}{2}} + \eta^{n+\frac{1}{2}}\right\|_0 + h^k\right). \quad (50)$$

When $C \in H^3\left(0, T; H^{k+1}(\Omega) \cap W^{1,\infty}(\Omega)\right)$ and $p \in H^{k+1}(\Omega) \cap W^{1,\infty}(\Omega)$, by (12), (13) and corollary 3.1, the choice of constant K in (50) is possible. Let $v_h = \xi^{n+\frac{1}{2}}$, $G_{11} \le K\left(\left\|\xi^{n+\frac{1}{2}}\right\|_0^2 + \epsilon\left\|\nabla\xi^{n+\frac{1}{2}}\right\|_0^2 + \left\|\eta^{n+\frac{1}{2}}\right\|_0^2 + \left\|\nabla\eta^{n+\frac{1}{2}}\right\|_0^2 + h^{2k} + O(\Delta t)^4\right)$. Apply Taylor's expansion to G_2, G_3, G_6 and G_9; and apply (50) similarly to G_1 and G_8. Keep only G_5 and G_7 on the left hand side and neglect all the constants. Now (48) can be written as the following inequality:

$$\left\|\partial_t\xi^{n+\frac{1}{2}}\right\|_0\left\|\xi^{n+\frac{1}{2}}\right\|_0 + \left\|\nabla\xi^{n+\frac{1}{2}}\right\|_0^2 \le \left\|\xi^{n+\frac{1}{2}}\right\|_0^2 + \epsilon\left\|\nabla\xi^{n+\frac{1}{2}}\right\|_0^2 + \left\|\eta^{n+\frac{1}{2}}\right\|_0^2 + \left\|\nabla\eta^{n+\frac{1}{2}}\right\|_0^2 + h^{2k} + O(\Delta t)^4. \quad (51)$$

Take the sum from 0 to M on both side, $0 \le M \le N-1$. By using the telescoping skill and ϵ-inequality, (51) becomes:

$$\frac{1}{2\Delta t}\left(\left\|\xi^{M+1}\right\|_0^2 - \left\|\xi^0\right\|_0^2\right) + \sum_{n=0}^{M}\left\|\nabla\xi^{n+\frac{1}{2}}\right\|_0^2 \le K\sum_{n=0}^{M}\left(\left\|\xi^{n+\frac{1}{2}}\right\|_0^2 + \left\|\eta^{n+\frac{1}{2}}\right\|_0^2 + \left\|\nabla\eta^{n+\frac{1}{2}}\right\|_0^2 + (\Delta t)^4 + h^{2k}\right) + \epsilon\sum_{n=0}^{M}\left\|\nabla\xi^{n+\frac{1}{2}}\right\|_0^2. \quad (52)$$

Since $\sum_{n=0}^{M}\left\|\xi^{n+\frac{1}{2}}\right\|_0^2 = \sum_{n=0}^{M+1}\|\xi^n\|_0^2$, use Gronwall's inequality,

$$\left(\left\|\xi^{M+1}\right\|_0 + \sqrt{\sum_{n=0}^{M+1}\|\nabla\xi^n\|_0^2}\right)^2 \le \left\|\xi^{M+1}\right\|_0^2 + \sum_{n=0}^{M+1}\|\nabla\xi^n\|_0^2 \le K\left(h^{2k} + (\Delta t)^4 + \left\|\xi^0\right\|_0^2\right). \quad (53)$$

Because u_0 is given, one can pick $u_{h,0}$ to approximate u_0 such that $\left\|u_0 - u_{h,0}\right\|_0 \le Ch^{k+1}$, thus $\left\|\xi^0\right\|_0 \le Ch^{k+1}$. One example is to let $u_{h,0}$ be the interpolation of u_0. Furthermore, let $J = M+1$, $\left\|\xi^J\right\|_0 + K\sqrt{\sum_{n=0}^{J}\|\nabla\xi^n\|_0^2} \le K\left(h^k + (\Delta t)^2\right)$. Therefore,

$$\|(W - W_h)_J\|_{L^2} + \left(\sum_{n=0}^{J}\|(W - W_h)_n\|_{H^1}^2\right)^{\frac{1}{2}} \le K\left(h^k + (\Delta t)^2\right). \tag{54}$$

Lemma 4.1. *[18] Suppose $p \in H^{k+1}(\Omega)$, and $1 \le J \le N$, then*

$$\left\|(p - p_h)_J\right\|_{L^2} + h\left\|(p - p_h)_J\right\|_{H^1} \le Kh^{k+1}. \tag{55}$$

Theorem 4.1. *Suppose $p \in H^{k+1}(\Omega) \cap W^{1,\infty}(\Omega)$, $C \in H^3\left(0, T; H^{k+1}(\Omega) \cap W^{1,\infty}(\Omega)\right)$, $W = \int_0^C D(\omega)d\omega$, $k > 1$ and $1 \le J \le N$. With (12) and (13), the numerical solution of (11) generated by (47) has error estimates as follows:*

$$\left\|(p - p_h)_J\right\|_{L^2} + h\left\|(p - p_h)_J\right\|_{H^1} \le Kh^{k+1}, \tag{56}$$

and

$$\|(C - C_h)_J\|_{L^2} + \left(\sum_{n=0}^{J}\|(C - C_h)_n\|_{H^1}^2\right)^{\frac{1}{2}} \le K\left(h^k + (\Delta t)^2\right). \tag{57}$$

Acknowledgments

M. He was supported by NSFC (Grants No.11101311), P. Sun was supported by NSF DMS-0913757.

References

[1] C. Wang, Fundamental models for fuel cell engineering, Journal of the Electrochemical Society 104 (2004) 4727–4766.
[2] Y. Wang, C. Wang, Transient analysis of polymer electrolyte fuel cells, Electrochimica Acta 50 (2005) 1307–1315.
[3] S. Um, C. Wang, Three-dimensional analysis of transport and electrochemical reaction in polymer electrolyte fuel cells, Journal of Power Sources 124 (2004) 40–51.
[4] Z. Wang, C. Wang, K. Chen, Two-phase flow and transport in the air cathode of proton exchange membrane fuel cells, Journal of Power Sources 94 (2001) 40–50.
[5] Y. wang, S. Basu, C. Wang, Modeling two-phase flow in PEM fuel cell channels, Journal of Power Sources 179 (2008) 603–617.
[6] T. V. Nguyen, R. E. White, A water and heat management model for proton-exchange-membrane fuel cells, Electrochem Soc 140 (1993) 2178–2186.
[7] S. Um, C. Wang, Computational study of water transport in proton exchange membrane fuel cells, Journal of Power Sources 156 (2006) 211–223.
[8] J. H. Nam, M. Kaviany, Effective diffusivity and water-saturation distribution in single-and two-layer pemfc diffusion medium, International Journal of Heat and Mass Transfer 46 (2003) 4595–4611.
[9] P. Sun, S. Zhou, Q. Hu, G. Liang, Numerical study of a 3D two-phase pem fuel cell odel via a novel automated finite element/finite volume program generator, Communications in Computational Physics 11 (2012) 65–98.
[10] P. Sun, G. Xue, C. Wang, J. Xu, A domain decomposition method for two-phase transport model in the cathode of a polymer electrolyte fuel cell, Journal of Computational Physics 228 (2009) 6016–6036.
[11] P. Sun, G. Xue, C. Wang, J. Xu, Fast numerical simulation of two-phase transport model in the cathode of a polymer electrolyte fuel cell, Communications in Computational Physics 6 (2009) 49–71.
[12] P. Sun, G. Xue, C. Wang, J. Xu, A combined finite element-upwind finite volume-newton's method for liquid feed direct methanol fuel cell simulations, in: Engineering, T. Conference (Eds.), Proceeding of Sixth International Fuel Cell Science, 2008, pp. 851–864.
[13] P. Sun, Modeling studies and efficient numerical methods for proton exchange membrane fuel cell, Computer Methods in Applied Mechanics and Engineering 200 (2011) 3324–3340.
[14] T. Arbogast, M. Wheeler, N. Zhang, A nonlinear mixed finite element method for a degenerate parabolic equation arising in flow in porous media, SIAM Society for Industrial and Applied Mathematics 33 (1996) 1669–1687.
[15] N. Eyres, D. Hartree, J. Ingham, R. Jackson, The calculation of variable heat flow in solids, Philosophical Transactions of the Royal Society A240 (1946) 1–57.
[16] M. Rose, Numerical methods for flows through porous media, Mathematics of Computation 40 (1983) 435–467.
[17] C. Wang, P. Cheng, A multiphase mixture model for multiphase, multicomponent transport in capillary porous media I. Model development, International Journal of Heat and Mass Transfer 39 (1996) 3607–3618.
[18] P. G. Ciarlet, The Finite Element Method for Elliptic Problems, North-holland, New York, 2002.